



METHODS OF PROBABILISTIC TSUNAMI HAZARD ANALYSIS IN SOUTH CHINA SEA IMPACTED BY LOCAL POTENTIAL SOURCES

Y.F. Ren⁽¹⁾, P. Zhang⁽²⁾, R.Z. Wen⁽³⁾

⁽¹⁾ Associate Professor, Institute of Engineering Mechanics, China Earthquake Administration, renyefei@iem.ac.cn

⁽²⁾ Postgraduate, Institute of Engineering Mechanics, China Earthquake Administration, weihaojg@sina.com

⁽³⁾ Professor, Institute of Engineering Mechanics, China Earthquake Administration, ruizhi@iem.ac.cn

Abstract

The South China Sea (SCS) is recognized as an area at high risk of tsunamis. The Manila Trench has long been considered as the regional source of tsunamis that might affect Chinese coastal areas, and considerable analysis of the tsunami hazard has been conducted in this area. However, there has been no consideration of other potential local sources near the coastal area. Thus, the locations of local potential tsunami sources (PTs) along the southern coast of China and the evaluation of their impact on tsunami hazard assessment require investigation. We identified eight local PTs for given seismic activity parameters. For the probabilistic tsunami hazard analysis (PTHA), the lower-limit earthquake magnitude was determined as 7.0, based on numerical simulation of tsunami scenarios. Two targeted sites in the Pearl River Estuary and Taiwan Strait were selected for PTHA, which were referenced to Hong Kong and Xiamen. The annual rate of tsunami waves exceeding a given height ($h \geq H$) was calculated for each site. The results show that the upper-limit earthquake magnitude is an important factor in the PTHA computation. The probabilities of tsunami waves exceeding a given height ($h \geq H$) within 100 years and their return periods were calculated for each site. The results show that the probability of $h \geq 0.5$ m within 100 years is 40% in Xiamen but only 10% in Hong Kong. If the Manila Trench were considered as a regional source, these probabilities would be higher. It is concluded that the tsunami hazard on the southern coast of China is very high and that both regional and local PTs should be included in any future PTHA.

Keywords: PTHA; Potential local tsunami source; Seismic activity; Numerical simulation; South China Sea

1. Introduction

In ancient Chinese literature, the word “haiyi” or “chaoyong” is used to describe any abnormal rise and fall of sea level. This makes it difficult to distinguish between tsunami and storm-surge events in historical records, and it can lead to the misapprehension that few tsunamis have affected China in the past [1]. Coastal areas of China have not been affected by any destructive tsunamis during the last 100 years and consideration of the tsunami hazard has been neglected. However, the 2004 Sumatra and 2011 Tohoku earthquakes and tsunamis caused considerable numbers of casualties and large economic losses, which raised the awareness of the Chinese government and population to the danger posed by tsunamis.

The Pearl River Delta economic circle in Southeast China, which includes major cities such as Hong Kong, Macau, and Shenzhen, comprises part of the most economically developed area of the country. Coastal areas such as Fuzhou, Quanzhou, and Xiamen are also developed based on economic exchange with Taiwan. The increasingly important major infrastructure projects, such as the Hong Kong–Zhuhai–Macao Bridge, and the Dayawan and Yangjiang nuclear power plants have been built or are planned to be built along the coastline. Therefore, it is imperative that a comprehensive evaluation of the tsunami hazard in this area be undertaken. Assessments of the tsunami hazard in the South China Sea (SCS) have been performed in recent years by both Chinese scientists [e.g., 2] and international researchers [e.g., 3]. However, these studies have focused mostly on



the potential tsunami hazard by considering the regional source as the Manila Trench; the influence from any other local source along the Chinese coast has been largely overlooked. Some studies have shown that the seismic tectonics of the Chinese coastal area of the SCS could trigger a destructive tsunami [4, 5]. Historical records have revealed that some destructive earthquakes have occurred within this area, which then triggered damaging tsunamis [1]. For example, the $M7.5$ earthquake on December 19, 1604 in Quanzhou (Fujian Province) and the $M7.3$ earthquake on February 13, 1918 in Shantou (Guangdong Province) both generated tsunami waves.

Given the socioeconomic importance of Southeast China, the locations of local potential tsunami sources (PTSs) along the southern coast and the evaluation of their impact on tsunami hazard require investigation. In this study, we identified eight local PTSs for given seismic activity parameters, and with reference to the method of probabilistic seismic hazard analysis, the method of probabilistic tsunami hazard analysis (PTHA) was used for the investigation. The probabilities of tsunami waves exceeding a given height were calculated for some typical sites within the Pearl River Delta and Taiwan Strait region. The results reported in this paper provide scientific support for further studies of the effects of local sources on probabilistic tsunami hazard analyses of the southern coastal area of China.

2. Potential Tsunami Sources (PTSs)

The Manila Trench is where the Eurasian Plate is subducting beneath the Philippine Plate and it is a region of frequent earthquakes, which have elevated concern regarding the tsunami hazard in the SCS. Consequently, most previous studies have focused on the Manila Trench as the regional PTS, rather than PTSs along the Chinese coast.

In June 2015, the fifth-generation national “Seismic ground motion parameters zonation map of China (GB 18306-2015)” was issued. It delineated 1206 potential seismic sources (PSSs) across the entire country and in some neighboring areas. Among these PSSs, 15 were selected as local PTSs by [1] and [6] depending on the upper-limit earthquake magnitude, seismic tectonic setting, seismic activity, and other parameters. Of the 15, 8 in the SCS (Nos. 8–15; Fig. 1) were selected for consideration in this study. It should be noted that only those PSSs located within the Taiwan Strait were selected for this study, rather than those located to the east of Taiwan. This was because it is believed that Taiwan protects the Chinese mainland from the effects of tsunamis generated to the east. Fig. 1 also shows the six regional PTSs (Nos. RM1–RM6) in the Manila Trench, as given by [1]. Because this study considered only the roles of local PTSs, the importance of the combination of both local and regional PTSs to the PTHA will be discussed in further study.

Table 1 presents the geographical locations and earthquake source parameters of the eight PTSs used for the PTHA. For the PTHA, it is necessary to know the parameters of the upper limit of the earthquake magnitude M_u , constant b in the Gutenberg–Richter law, and the annual rate of occurrence of an earthquake ν , which will be discussed in the following text.

3. Numerical Simulation of Tsunami Scenarios

Before conducting the PTHA for the local sources, we performed numerical simulations of the propagation processes of two tsunami scenarios to analyze the characteristics of each local source. In this study, only the effects of source 13 are illustrated, because it affects both sites #1 and #2. Due to its directionality, it is unlikely that PTS 13 will dominate the PTHA for either location, but Figure 1 illustrates why it needs to be included for both sites. The two scenarios involved modeling earthquake magnitudes of $M_w 7.0$ and $M_w 7.5$ at PTS site No. 13. The value of $M_w 7.5$ is the upper-limit earthquake magnitude of this PTS (see Table 1).

The ruptured length and width of the fault were determined from empirical relationships given by [7], which are scaled according to the magnitude. [7] also developed an empirical relationship between the magnitude and average slip, but this correlation coefficient is only 0.1 (see Table 2B of [7]). Therefore, the average slip in this study was estimated using the following equation [8]:



$$M_0 = \mu LWD \quad (1)$$

where M_0 is the scalar moment of the earthquake, coefficient μ is the shear rigidity of the Earth's crust, L and W represent the length and width of the fault plane, respectively, and D is the amount of average slip. Parameter μ is related to the density ρ and shear velocity V_S of the Earth's crust:

$$V_S = \sqrt{\frac{\mu}{\rho}} \quad (2)$$

Usually the mean values of ρ and V_S of the shallow crust are estimated as 2.7 g/cm³ and 3.6 km/s, respectively, for the Chinese mainland [9]. Consequently, μ is equal to 35 Gpa based on the above formulas.

Table 1 – Locations and earthquake source parameters of the eight local PTSs affecting the Chinese coastal area of the SCS

No.	Name	Node location			Strike (°)	Length (km)	Width (km)	Average depth (km)	Dip (°)	Rake (°)	Upper-limit magnitude (M_w)
		Node	Lon. (°E)	Lat. (°N)							
8	Quanzhou	Q1	119.01	24.54	65	92	71	20	60	90	8.0
		Q2	119.83	24.93							
9	Xiamen No.1	XM1	118.77	24.00	58	51	71	20	60	90	8.0
		XM2	119.18	24.26							
10	Xiamen No.2	XM3	118.43	23.74	57	74	71	20	60	90	8.0
		XM4	118.67	23.91							
		XM5	119.04	24.12							
11	Xiamen No.3	XM6	118.52	23.68	53	59	71	20	60	90	8.0
		XM7	118.97	24.03							
12	Nan'ao	BN1	117.03	23.03	47	75	50	20	60	90	7.5
		BN2	117.54	23.51							
13	Taiwan	TW1	116.61	22.61	118	130	50	20	60	90	7.5
		TW2	116.84	22.61							
		TW3	116.98	22.56							
		TW4	117.18	22.47							
		TW5	117.55	22.32							
		TW6	117.77	22.22							
		TW7	117.78	22.22							
14	Zhu-Ao	ZA1	114.11	21.87	74	52	50	20	60	90	7.5
		ZA2	114.25	21.95							
		ZA3	114.43	21.99							
		ZA4	114.59	22.00							
15	Dan'gan	DG1	113.45	21.41	63	135	50	20	60	90	7.5
		DG2	113.83	21.63							
		DG3	114.21	21.84							
		DG4	114.59	21.98							

The open-source Cornell Multi-grid Coupled Tsunami Model is commonly used for simulations [12]. Here, the linear shallow-water wave equation was employed rather than the nonlinear model. The linear treatment can serve our purposes sufficiently, as has been verified already by [2]. A run-up stage was not included in this study. More than 1200 targeted sites were selected from the 10-m isobath along the Chinese coast. Fig. 2 show the distribution of simulated wave height associated with each scenario for PTS No. 13.

In this study a uniform slip distribution is considered, i.e., same values of D elsewhere on the earthquake fault zone. However, a number of studies of past tsunamis, in particular the Tohoku Tsunami, indicated that the slip distribution can have a significant effect on the tsunami wave magnitude [10]. This is particularly true for

near-source tsunamis such as in this study. However, as the complexity and heterogeneous of fault rupture, more scenarios in PTHA computation needs to be considered. Because of the limited capacity for the computation, only uniform slip distribution is considered in this study.

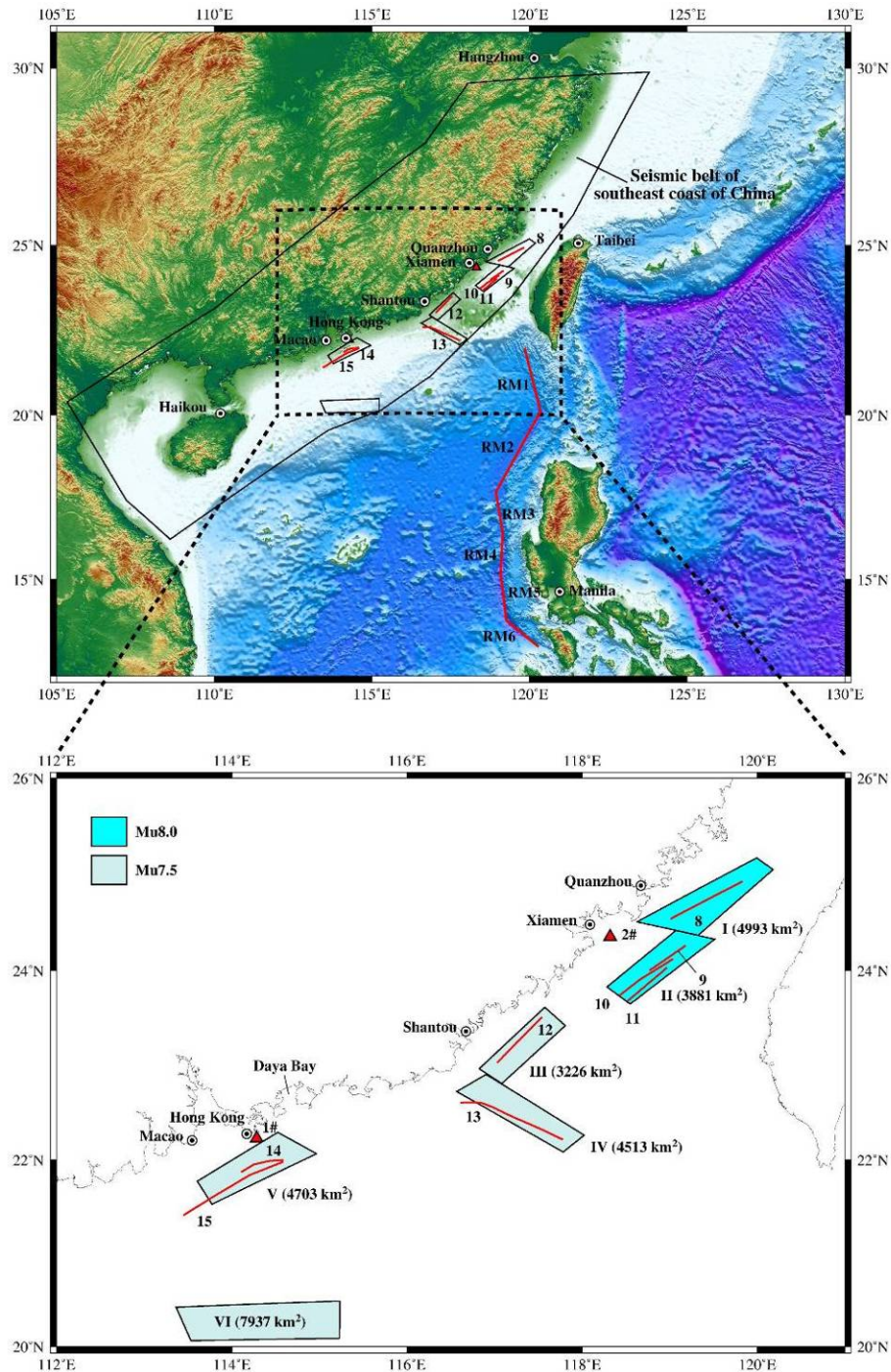


Fig. 1 – Local and regional potential tsunami sources (PTSS) affecting the Chinese coastal area of the South China Sea. Regional PTSS RM1–RM6 were derived from [1]. Local PTSS (Nos. 8–15) were determined by [1] and [6]. The polygon defines the seismic belt of the southeast coast of China, which was used for calculating the parameters of seismic activity for each PSS. The six quadrilaterals delineate the PSSs identified by the seismic ground motion parameter zonation map of China. The areas of the PSSs are marked in parentheses. The upper limits of the earthquake magnitudes of the PSSs are indicated by different colors. Numbers 1# and 2# mean the locations where the PTHA was performed for the case studies in the following text.

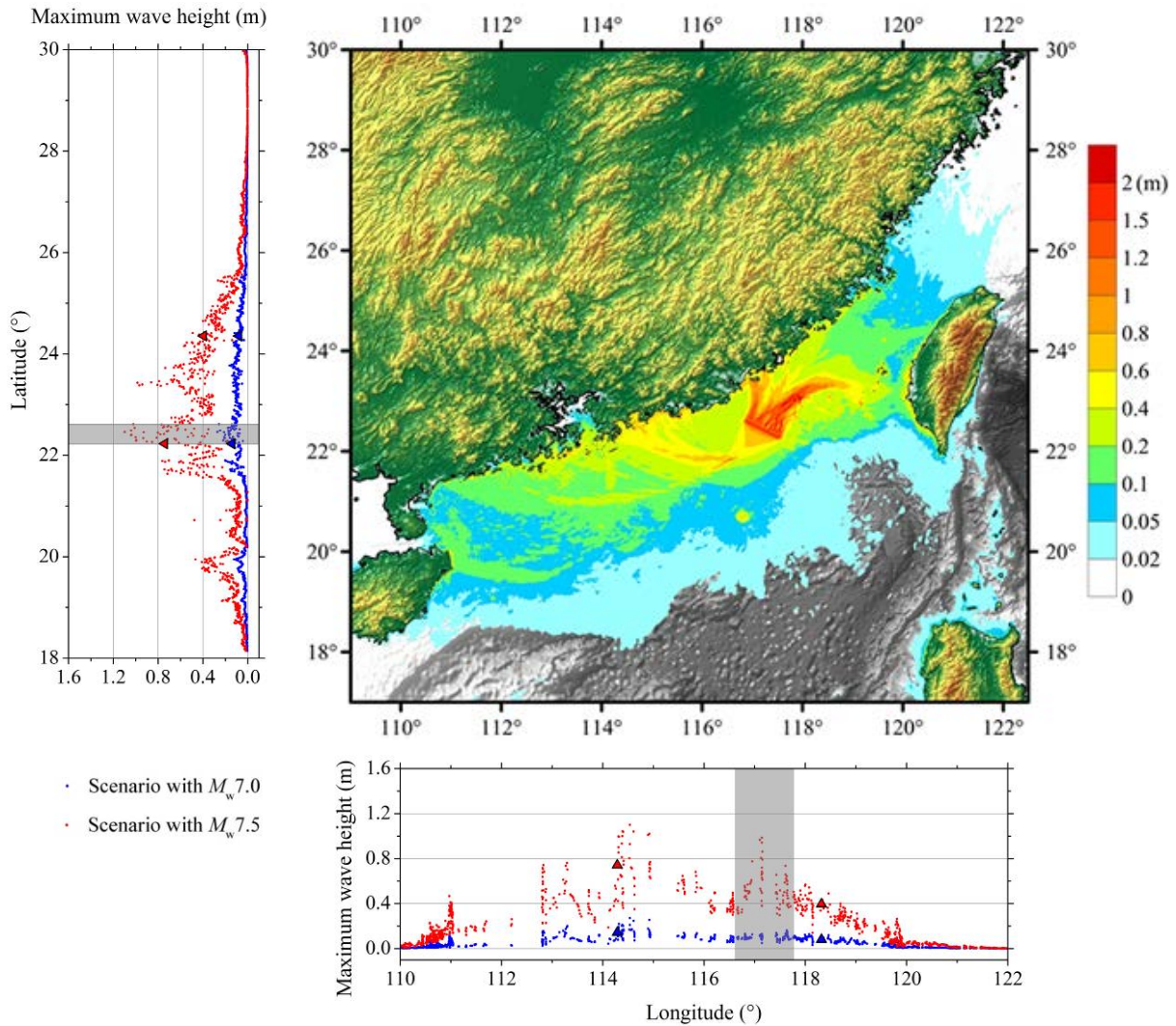


Fig. 2 – Tsunami wave heights along the Chinese coast when M_w 7.0 and M_w 7.5 scenario earthquakes occur at PTS No. 13. The middle figure presents the distribution of maximum wave height for the M_w 7.5 scenario. Shaded areas indicate the projection of PTS No. 13 at the corresponding longitude and latitude. Red and blue triangles show the wave heights at the two sites of interest for which the PTHA was conducted.

The value of M_0 can be determined using the following equation [11]:

$$M_w = \frac{2}{3} \log M_0 - 10.7 \quad (3)$$

where M_w is the moment magnitude of an earthquake; here, given as 7.0 and 7.5.

The maximum wave height at the targeted sites is estimated to be about 1.2 m for an M_w 7.5 earthquake at PTS No. 13 (Fig. 2). Although the wave height is low, PTS No. 13 affects a much wide region, not only in the Pearl River Estuary (where site 1# is located; see Fig. 1) but also in the Taiwan Strait (where site 2# is located; see Fig. 1). The reasonable explanation for this is that the fault strike is oblique to the coastline for PTS No. 13.

Fig. 2 show that for an M_w 7.0 earthquake occurring at PTS No. 13, the resulting tsunami wave heights at all sites are very small, i.e., mostly <0.2 m. Therefore, the lower-limit earthquake magnitude for each PTS is suggested to be 7.0 in the following PTHA.



4. PTHA Method

The concept and computational procedure of PTHA generally follows the method of probabilistic seismic hazard analysis developed originally by [13]. The procedure of probabilistic seismic hazard analysis has been used in China for the compilation of the zonation map of seismic ground motion parameters [14]. With reference to this procedure, we proposed the following method for PTHA in China.

For an earthquake occurring within a region, the cumulative distribution function (CDF) $F(M)$ and probability density function (PDF) $f(M)$ of its magnitude M can be expressed as:

$$F(M) = \frac{1 - \exp[-\beta(M - M_{\min})]}{1 - \exp[-\beta(M_{\max} - M_{\min})]}, \quad M_{\min} < M < M_{\max} \quad (4)$$

$$f(M) = \frac{\beta \exp[-\beta(M - M_{\min})]}{1 - \exp[-\beta(M_{\max} - M_{\min})]}, \quad M_{\min} < M < M_{\max} \quad (5)$$

where M_{\max} and M_{\min} are the possible maximum and minimum magnitudes for an earthquake occurring within this region, $\beta = b \times \ln 10$, and b is a statistical constant of the Gutenberg–Richter recurrence law.

Suppose N_i earthquakes happen at the i -th PTS. Their spatial locations and magnitudes can be produced randomly using the Monte Carlo technique. The N_i magnitudes should meet the PDF (Eq. (5)) of this PTS. The value of M_{\max}^i should be the upper-limit earthquake magnitude M_{ui} of this PTS, i.e., 7.5 or 8.0 in this study (see Fig. 2), and the value of M_{\min}^i (7.0) is the lower-limit earthquake magnitude proposed previously. Here, we use M_1^i and M_2^i instead of M_{\min}^i and M_{\max}^i , respectively.

For the site of interest, N_i values of maximum wave height can be obtained by numerical simulation of the tsunami generation and propagation processes triggered by these N_i earthquakes. The length, width, and average slip of the fault plane for each earthquake occurring within the local PTSs were determined as discussed above. For an earthquake occurring in a regional PTS, e.g., the Manila Trench, it is suggested that these parameters be determined by empirical relationships given by [15] which are suitable for a subduction earthquake.

Based on the statistics of historical data, [16] found that tsunami wave heights follow a lognormal distribution. The PDF of tsunami wave height can be expressed as

$$f_i(h) = \frac{1}{\sqrt{2\pi}h\sigma} \exp\left(-\frac{[\ln(h) - \mu]^2}{2\sigma^2}\right) \quad (6)$$

where h is wave height, and μ and σ are the mean value and standard deviation of $\ln(h)$, respectively, which can be calculated using the N_i values of maximum wave height. Then, we can compute the CDF of the tsunami wave exceeding a given height H by taking the integral of the PDF:

$$F_i(h \geq H) = \int_H^{\infty} f_i(h) dh = \frac{1}{\sqrt{2\pi}\sigma} \int_H^{\infty} \exp\left(-\frac{[\ln(h) - \mu]^2}{2\sigma^2}\right) \frac{dh}{h} \quad (7)$$

If the annual rate of occurrence of earthquakes greater than M_1^i and less than M_2^i at the i -th PTS, i.e., $v_i(M_1^i \leq M \leq M_2^i)$, is known, the annual rate of occurrence of tsunami waves from the i -th PTS that exceed a given height H , i.e., $v_i(h \geq H)$, can be calculated as

$$v_i(h \geq H) = F_i(h \geq H) \cdot v_i(M_1^i \leq M \leq M_2^i) \quad (8)$$

The procedure to compute $v_i(M_1^i \leq M \leq M_2^i)$ is presented in the following text.

For sites of interest affected by multiple PTSs, the contributions from each PTS should be considered in combination:



$$v(h \geq H) = 1 - \prod_{i=1}^{N_T} [1 - v_i(h \geq H)] \quad (9)$$

where N_T is the total number of PTSs and $v(h \geq H)$ is the total result of the annual rate of $h \geq H$.

Therefore, the return period is

$$R(h \geq H) = \frac{1}{v(h \geq H)} \quad (10)$$

Under the assumption of the Poissonian occurrence of earthquakes, the probability of observing at least one event $h \geq H$ within period T is equal to

$$P(h \geq H, t = T) = 1 - \exp(-v(h \geq H) \cdot T) \quad (11)$$

5. Seismic Activity Parameters for PTHA

For PTHA, three input parameters must be known for each PTS: b_i , M_{ui} , and $v_i(M_1^i \leq M \leq M_2^i)$. These three parameters characterize the seismic activity within the region of each individual PTS and therefore, their values for a specific PTS are identical to those of the collocated PSS. Fig. 1 shows that the locations of the eight PTSs match the six PSSs expressed by the six quadrilaterals and marked by the Roman numerals. The areas of the delineated regions of each individual PSS are also presented in Fig. 1.

The upper-limit earthquake magnitudes for all 1206 PSSs are given in the Chinese national zonation map (Fig. 1) and Table 2 lists those for the six PSSs used in this study. Usually, the region of a single PSS is too small to collect adequate data on historical earthquake events for the analysis of seismicity; therefore, 29 seismic belts are delineated across China within this zonation map. Each seismic belt includes dozens of PSSs, but only one value of b_{belt} (value of b of the Gutenberg–Richter recurrence law within this belt) and v_{belt} (annual rate of occurrence of earthquakes $M \geq 4.0$ within this belt) is given for each belt based on a statistical analysis of historical events. The b_i value of each PSS is assumed to be directly equal to the corresponding b_{belt} , and v_{belt} is a sum of v_i of all included PSSs [14]. The six PSSs used in this study are all located within the seismic belt along the southeast coast of China (see Fig. 1), for which the values of $b_{\text{belt}} = 0.87$ and $v_{\text{belt}} = 5.6$ have been assigned [14].

The b_i value of each PSS was set to b_{belt} (0.87). The annual rate of occurrence of earthquakes associated with different levels of magnitude $v_i(M_j)$ can be calculated using the following equation [14]:

$$v_i(M_j) = v_{\text{belt}}(M_j) \cdot \gamma_i(M_j) \quad (12)$$

where M_j means the j -th level of discrete magnitudes ordered by $M_0 + (j-1) \cdot \Delta M \leq M_j \leq M_0 + j \cdot \Delta M$, $M_0 = 4.0$ (lower-limit earthquake magnitude for the seismic belt or each PSS), j equals an integer (here, expressed by Roman numerals), $1 \leq j \leq (M_{ui} - M_0) / \Delta M$, ΔM is the discrete interval given as 0.5 for small earthquakes and 0.3 or 0.2 for moderate and large earthquakes in the national zonation map, and $\gamma_i(M_j)$ is the weighting of the i -th PSS covering its attributed seismic belt, following the principle:

$$\sum_{i=1}^{N_{Sj}} \gamma_i(M_j) = 1 \quad (13)$$

where N_{Sj} means the number of PSSs at which earthquakes greater than M_j can occur. Determining the value of $\gamma_i(M_j)$ is complex, requiring eight factors that are both subjective and objective [14]. The seismic source area is one of the most important factors and therefore, we consider only this factor in the calculation of $\gamma_i(M_j)$ using the following equation:



$$\gamma_i(M_j) = \frac{A_i(M_j)}{\sum_{i=1}^{N_{Sj}} A_i(M_j)} \quad (14)$$

where $A_i(M_j)$ means the area of the i -th PSS.

In this study, $\Delta M = 0.5$ was set equal to the interval value of M_{ui} (see Fig. 1). Because M_1^i is determined as 7.0 and M_2^i is 7.5 or 8.0, there are only two levels for M_j within the range of M_1^i to M_2^i . Therefore, there are two levels (M_{VII} and M_{VIII}) for PSS Nos. I and II because of the upper-limit earthquake magnitude of 8.0 (see Fig. 1), and only one level (M_{VII}) for the other four PSSs ($M_u = 7.5$). The values of $\gamma_i(M_{VII})$ and $\gamma_i(M_{VIII})$ for the six PSSs in this study can be calculated using Eq. (14), as shown in Table 2.

For calculating $v_i(M_1^i \leq M \leq M_2^i)$, it is necessary to know the value of $v_{belt}(M_j)$ in Eq. (12), i.e., $v_{belt}(M_{VII})$ and $v_{belt}(M_{VIII})$. From Eq. (4), the probabilities of occurrence of magnitudes of M_{VII} and M_{VIII} are calculated as:

$$F_{belt}(M_{VII}) = F_{belt}(M = 7.5) - F_{belt}(M = 7.0) \quad (15)$$

$$F_{belt}(M_{VIII}) = F_{belt}(M = 8.0) - F_{belt}(M = 7.5) \quad (16)$$

where $\beta_{belt} = b_{belt} \times \ln 10 = 2.003$, $M_{max} = M_u = 7.5$ or 8.0, and $M_{min} = 4.0$. As a result, $F_{belt}(M_{VII}) = 1.554 \times 10^{-3}$ and $F_{belt}(M_{VIII}) = 5.706 \times 10^{-4}$. Then, $v_{belt}(M_{VII})$ can be calculated by

$$v_{belt}(M_{VII}) = F_{belt}(M_{VII}) \cdot v_{belt}(M \geq 4.0) \quad (17)$$

As a result, $v_{belt}(M_{VII}) = 8.7 \times 10^{-3}$. In the same way, $v_{belt}(M_{VIII}) = 3.196 \times 10^{-3}$.

From Eq. (12), $v_i(M_{VII})$ and $v_i(M_{VIII})$ can be calculated, as shown in Table 2.

Finally, the value of $v_i(M_1^i \leq M \leq M_2^i)$ can be calculated using the following equation:

$$v_i(M_1^i \leq M \leq M_2^i) = \begin{cases} v_i(M_{VII}) & M_{ui} = 7.5 \\ v_i(M_{VII}) + v_i(M_{VIII}) & M_{ui} = 8.0 \end{cases} \quad (18)$$

All of the results of $v_i(M_1^i \leq M \leq M_2^i)$ for each PSS are given in Table 2.

Table 2 – Parameters of seismic activity for each local PTS used in this study

No. of PSS	No. of PTS	Name of PTS	b_i	M_{ui}	$A_i(M_j)$ (km ²)	$\gamma_i(M_{VII})$	$\gamma_i(M_{VIII})$	$v_i(M_1^i \leq M \leq M_2^i)$ $\times 10^{-3}$		
								$v_i(M_{VII})$	$v_i(M_{VIII})$	Total
I	8	Quanzhou	0.87	8.0	4993	0.171	0.563	1.485	1.798	3.283
II	9	Xiamen No.1	0.87	8.0	3881	0.133	0.437	1.154	1.398	2.552
	10	Xiamen No.2								
	11	Xiamen No.3								
III	12	Nan'ao	0.87	7.5	3226	0.110	0.000	0.959	0.000	0.959
IV	13	Taiwan	0.87	7.5	4513	0.154	0.000	1.342	0.000	1.342
V	14	Zhu-Ao	0.87	7.5	4703	0.161	0.000	1.399	0.000	1.399
	15	Dan'gan								
VI				7.5	7937	0.271	0.000	2.361	0.000	2.361
Total					29253	1.000	1.000	8.700	3.196	11.896

6. Case Studies of the PTHA

Two typical targeted sites were selected from more than 1200 ones mentioned in previous numerical simulation of tsunami scenarios. One was located in the coastal area of the Pearl River Estuary numbered 1# and another

one was in the Taiwan Strait numbered 2#. Site 1# was referenced to Hong Kong City and site 2# to Xiamen City. Here, PTS Nos. 14 and 15 were selected for the PTHA as case studies for site 1#, PTS Nos. 8–12 were considered for sites 2# and PTS No. 13 was considered for both sites.

We randomly produced 50 scenario earthquakes for each PTS using the Monte Carlo technique. The epicenters were spaced randomly along the entire length of the fault. The magnitudes followed the corresponding PDFs of the individual PTSs. Fig. 3 shows the spatial distribution of the epicenters and CDF of the magnitudes associated with the 50 scenario earthquakes for PTS No. 15. It can be seen that the epicenters are distributed almost uniformly along the fault and that the magnitude distribution is almost consistent with the theoretical CDF curve. This indicates that the simulation is acceptable for PTS No. 15. With a greater number of scenarios, higher accuracy could be achieved; however, because of the limited capacity for the computation, only 50 simulations were conducted.

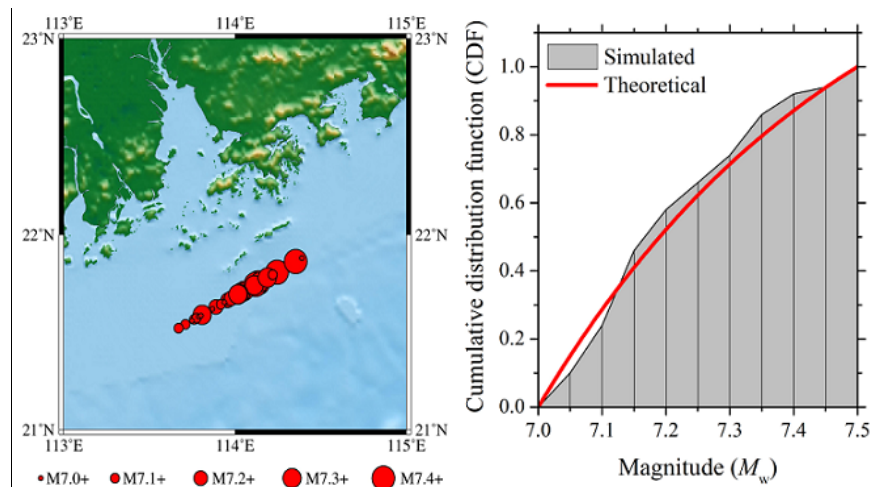


Fig. 3 – Locations of 50 earthquakes produced randomly using the Monte Carlo technique for PTS No. 15 (Left panel) and cumulative distribution function of the magnitudes of these earthquakes (Right panel).

The processes of tsunami generation and propagation were simulated numerically for 50 scenario earthquakes for each PTS using the estimates of rupture length, width, and average slip described previously. Using Eq. (6), the PDFs of the wave height at both sites were regressed for the 50 simulations for each PTS, as shown in Fig. 4. The regressed μ and σ are also shown in Fig. 4. The acceptable goodness of fit confirms the assumption that tsunami wave heights follow a lognormal distribution.

Using Eq. (8), the annual rates of occurrence of tsunami waves from each PTS exceeding a given height H were calculated for sites 1# and 2#, respectively, and the total rates of the combined contributions from all impacted PTSs were calculated using Eq. (9), as shown in Fig. 5.

Fig. 5 shows the total rate of occurrence at site 1# is predominantly attributed to PTS No. 14, site 2# to Nos. 9-11, respectively. It is dependent on the relative geographical position between the targeted site of interest and the PTS (see Fig. 1). It is noted that for the annual rate of occurrence at site 1#, when wave height is >1.0 m, the contribution from PTS No. 14 is decreased, while that from PTS No. 15 is increased. In fact, the wave height at site 1# is <1.0 m if the tsunami is generated at PTS No. 15 (see Fig. 3). The PDFs of wave height >1.0 m were estimated by extrapolation of the data <1.0 m. Future work will confirm whether this is correct; it might be better to have a truncation at a wave height of 1.0 m.

The annual rate of occurrence of tsunami waves exceeding 0.5 m is 8×10^{-4} at site 1#, almost smaller by one order of magnitude than at site 2# which is 6×10^{-3} . A possible reason for this is that the upper-limit earthquake magnitude at PTS No. 14 is 7.5, which is the major contributor for site 1#, whereas it is 8.0 for PTS Nos. 9–11 (site 2#).

For both sites, we calculated both the return period of the occurrence of tsunami waves exceeding a given height using Eq. (10) and the probability of exceeding a given tsunami wave height within 100 years using Eq.



(11); the results are presented in Fig. 6. For a wave height <0.1 m, the probability for site 1# is 35%, smaller than the value of about 75% for site 2#. This is because only three PTSs were considered in the hazard analysis for sites 1# (see Fig. 4(a)), whereas six PTSs were considered in the analysis for site 2# (see Fig. 4(b)). For low-height wave (e.g., 0.1 m), the CDFs are almost approaching to 1.0 for each PTSs. Due to a similar level of annual rate of occurrence of earthquakes for each PTS (Table 2), the probability of exceeding a given tsunami wave height for a targeted site, the numbers of contributing PTSs are the most dependent factor.

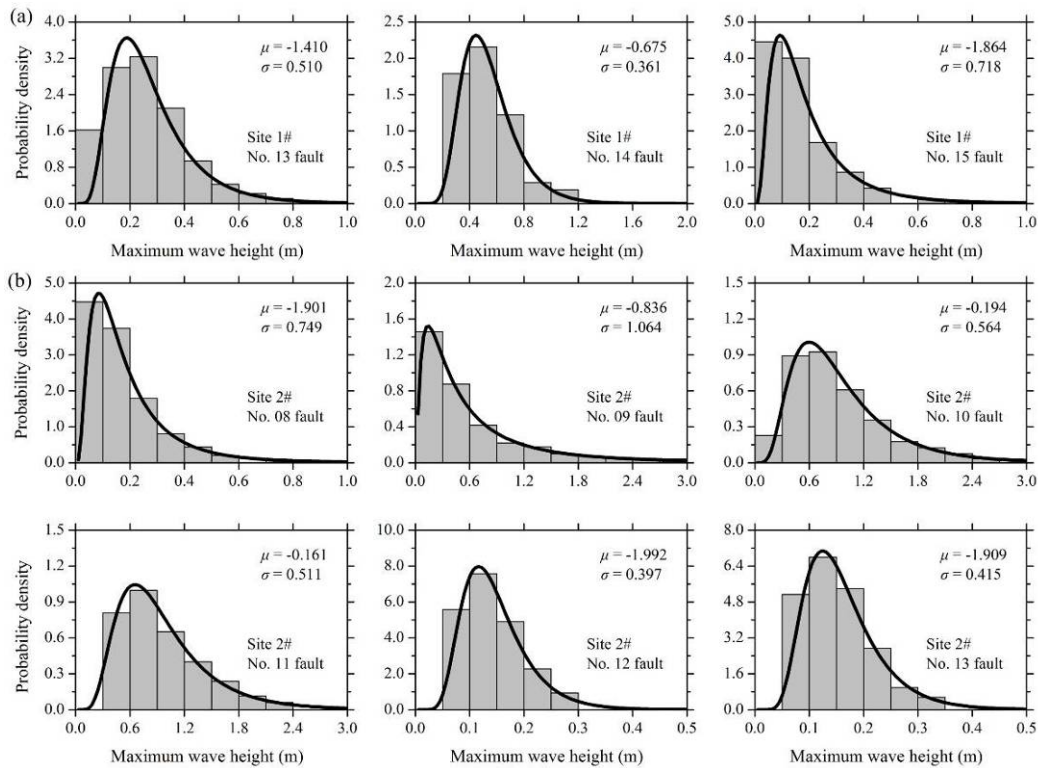


Fig. 4 – Regressed probability density functions (PDFs) of the 50 maximum tsunami wave heights for site 1# induced by the 50 scenario earthquakes at PTS Nos. 13–15, and site 2# by PTS Nos. 8-13. Thick curves represent the regressed PDFs. Grey bars represent discrete PDFs calculated using the regressed μ and σ .

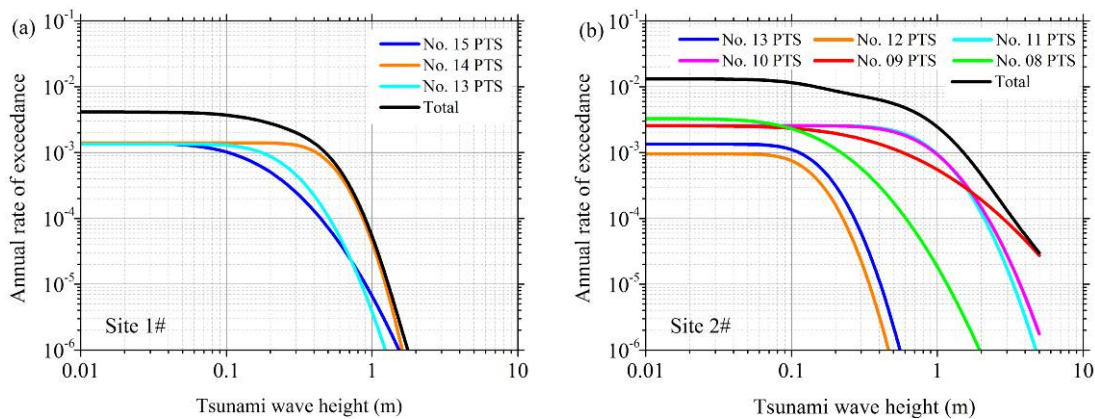


Fig. 5 – Annual rate of occurrence of tsunami waves exceeding a given height at sites 1# and 2#, including the results attributed to the individual PTSs and a synthesis of all the PTSs

As mentioned above, site 1# was referenced to Hong Kong City and site 2# to Xiamen City. Fig. 6 shows that the probability is 10% in Hong Kong, but 40% in Xiamen for tsunami waves >0.5 m. The probabilities of site 2# are much higher than site 1# for waves >1.0 m, almost higher by two orders of magnitude. The upper-limit earthquake magnitude of PTS Nos. 9–11 is 8.0 and these sources have the greatest impact on sites 2. The



upper-limit earthquake magnitude of PTS Nos. 12–15 is 7.5 and these sources have the greatest impact on sites 1#. As expected, it shows that the upper-limit earthquake magnitude of the PTS plays an important role when assessing the tsunami hazard.

As Fig. 6 shows, the return period of tsunami waves >0.5 m is >1000 years for Hong Kong, but only >200 years for Xiamen, 400 years even for waves >1.0 m. Compared with Xiamen in the Taiwan Strait, the tsunami hazard at Hong Kong in the Pearl River Estuary is much lower. It should be noted that only local PTSs were considered in this study. If the impact of the Manila Trench were also considered, the return periods calculated in this study for both sites would be shortened significantly and the probabilities would be greatly increased.

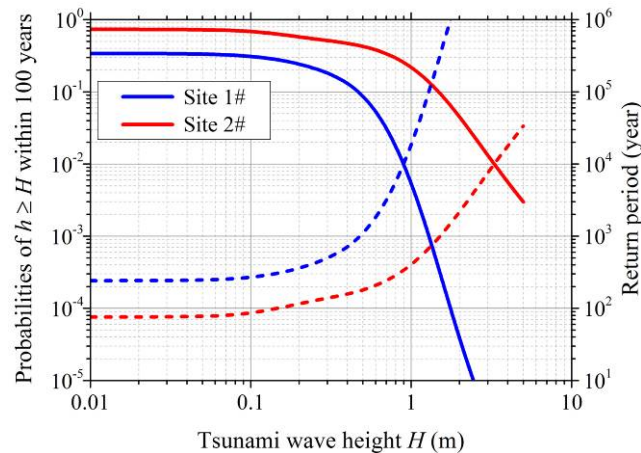


Fig. 6 – Probabilities of at least one occurrence of exceedance of tsunami wave height within 100 years for sites 1# and 2# (solid lines). Dashed lines show the return period for both sites where tsunami waves reach any level of tsunami wave height.

7 Conclusions

To apply a probabilistic tsunami hazard analysis (PTHA) to the Chinese coastal area we delineated some local potential tsunami sources (PTSs), determined some parameters of seismic activity for each source, and selected two typical targeted sites for case studies to demonstrate the proposed Chinese PTHA. Based on the results, the following conclusions were drawn:

(1) Using the data from the latest issued national “Seismic ground motion parameters zonation map of China (GB 18306-2015),” eight PTSs, Nos. 8–15, were delineated and the parameters of their seismic activity were determined, including the upper-limit earthquake magnitude M_u , the value of constant b of the Gutenberg–Richter recurrence law, and the annual rate of earthquake occurrence ν .

(2) Two targeted sites were selected in the Pearl River Estuary and the Taiwan Strait for use as PTHA case studies. They were referenced to Hong Kong and Xiamen, which are located close to these sites. For each site, the annual rate of occurrence of tsunami waves exceeding a given height was calculated, including that attributed to the individual PTSs and to a synthesis of all the PTSs. The comparison of results between two sites shows that the upper-limit earthquake magnitude of the PTSs is an important factor that affect the PTHA.

(3) Finally, the probabilities of at least one occurrence within 100 years and the return periods of tsunami waves exceeding a given height were calculated for both sites. The results showed that the probability was 10% in Hong Kong, but 40% in Xiamen for tsunami waves >0.5 m. The return periods was only 400 years in Xiamen for tsunami waves >1.0 m. If the Manila Trench was also considered as a regional source, the return periods would be shortened and the probabilities increased. It is concluded that the tsunami hazard for the southern coast of China is very high, and that both local and regional PTSs should be included in any future PTHA.

Noting that there is no consideration of uncertainty in any of the variables assumed for PTHA analysis in this study. As we know, there is significant uncertainty in the earthquake magnitude, slip distribution, tsunami wave generation, etc., that should be considered to establish a reliable probability of exceedance without



underestimating the potential tsunami wave heights. We will focus on this part of work in the further study and a logic tree method might be considered to be used.

Acknowledgements

This work is supported by the National Natural Science Fund No. 51278473, the Environmental Protection Research Fund for Public Interest No. 201209040 and the northeast Asia (China-Japan-Korea) cooperative research project of earthquake, tsunami and volcano No. ZRH2014-11. We would like to thank Dr. Xiaoming Wang for providing help with the COMCOT model.

References

- [1] Ren YF, Wen RZ and Song YY (2014): Recent progress of tsunami hazard mitigation in China. *Episodes* **37**(4), 277-283.
- [2] Liu Y, Santos A, Wang SM, Shi YL, Liu HL et al. (2007): Tsunami hazards along Chinese coast from potential earthquakes in South China Sea. *Physics of the Earth and Planetary Interiors*, **163**(4), 233-244.
- [3] Wu TR and Huang HC (2009): Modeling tsunami hazards from Manila trench to Taiwan. *Journal of Asian Earth Sciences*, **36**(1), 21-28.
- [4] Zhang HN (1995): Seismic activity and regional stability for the South China Sea and its surrounding area. *Acta Oceanologica Sinaca*, **17**(6), 81-89. (in Chinese)
- [5] Yang ML and Wei BL (2005): The Potential Seismic Tsunami Risk in South China Sea and it's Surrounding Region. *Journal of Catastrophology*, **20**(3), 41-47. (in Chinese)
- [6] Chen GX and Zhou BG (2011): Determination of seismic belts and potential seismic sources in China and its surrounding area. *Technique report of the seismic ground motion parameter zonation map of China*, China Earthquake Administration. (in Chinese)
- [7] Wells DL and Coppersmith KJ (1994): New empirical relationships among magnitude, rupture length, rupture width, rupture area, and surface displacement. *Bulletin of the Seismological Society of America*, **84**(4), 974-1002.
- [8] Aki K (1966): Generation and propagation of G waves from the Niigata earthquake of June 14, 1964. Part 2, Estimation of earthquake moment, released energy and stress-strain drop from G wave spectrum. *Bulletin of the Earthquake Research Institute*, **44**, 73-88.
- [9] Pei SP, Xu ZH and Wang SY (2004): Sn wave tomography in the uppermost mantle beneath the China continent and adjacent regions. *Chinese Journal of Geophysics*, **47**(2), 250-256. (in Chinese)
- [10] Ulutas E (2013): Comparison of the seafloor displacement from uniform and non-uniform slip models on tsunami simulation of the 2011 Tohoku–Oki earthquake. *Journal of Asian Earth Sciences*, **62**, 568-585.
- [11] Hanks TC and Kanamori H (1979): A Moment magnitude scale. *Journal of Geophysical Research*, **84**(B5), 2348-2350.
- [12] Liu PLF, Yong-Sik C, Briggs MJ, Kanoglu U and Synolakis CE: (1995) Runup of solitary waves on a circular island. *Journal of Fluid Mechanics*, **302**, 259-285.
- [13] Cornell CA (1968): Engineering seismic risk analysis. *Bulletin of the Seismological Society of America*, **58**(5), 1583-1606.
- [14] Gao MT (2015): *Manual for national code “Seismic ground motion parameters zonation map of China (GB 18306—2015)”*. Standards Press of China, Beijing.



- [15] Papazachos BC, Scordilis EM, Panagiotopoulos DG, Papazachos CB and Karakaisis GF (2004): Global Relations between Seismic Fault Parameters and Moment Magnitude of Earthquakes. *Bulletin of the Geological Society of Greece*, **36**, 1482-1489.
- [16] Choi BH, Pelinovsky E, Ryabov I and Hong SJ (2002): Distribution functions of tsunami wave heights. *Natural Hazards*, **25**(1), 1-21.